Applied Environmental Research

Volume 43 | Number 1 Article 1

2021-01-01

Change in Rainfall Patterns in the Hilly Region of Uttarakhand due to the Impact of Climate Change

Dilip Kumar

Rajib K. Bhattacharjya

Applied Environmental Research

Journal homepage : http://www.tci-thaijo.org/index.php/aer

Change in Rainfall Patterns in the Hilly Region of Uttarakhand due to the Impact of Climate Change

Dilip Kumar, Rajib Kumar Bhattacharjya*

Department of Civil Engineering, Indian Institute of Technology Guwahati, Assam, India
* Corresponding author: Email: rkbc@iitg.ac.in

Article History
Submitted: 21 April 2020/ Revision received: 18 July 2020/ Accepted: 20 July 2020/ Published online: 18 November 2020

Abstract

Uttarakhand, a Himalayan state of India, may experience an increase in temperature of 1.4°C to 5.8°C by 2100 due to global warming. The rise in temperature may melt the glaciers of the state and may have some significant impact on the rainfall. In this study, we have quantified the changes in the rainfall of the state. Also, an attempt has been made to evaluate the impact of climate change on rainfall. The future rainfall can be estimated by using a global circulation model (GCM). However, due to the very coarse spatial resolution of the different GCM, we cannot use them directly. For matching this spatial inequality between the GCM output and historical precipitation data, we used the statistical downscaling technique. In the present study, we have examined the suitability of the artificial neural network with principal component analysis for downscaling the rainfall for different hilly districts of the state. We used the GCM model developed by Canadian Earth System Model, and the Indian metrological department gridded rainfall data. We performed the analysis for the different scenarios to visualize the impact of climate change on rainfall trends for all nine hilly districts of Uttarakhand. Results show that there was a clear indication of climate change in upper Himalayan Districts like Pithoragarh, Rudraprayag, and Chamoli, which was observed from the peak of monthly rainfall. The percentage change of monsoon rainfall in the future may go up to 200 % in the case of RCP8.5, and the change maybe around 180% for RCP4. Also, the volume of rainfall may increase in the case of RCP8.5 from July to September as compared to the historical data, *i.e.*, there may be a shifting of monsoon rainfall in the future.

Keywords: Downscaling; Climate change; Rainfall; ANN; Scenario; PCA

Introduction

Uttarakhand is a Himalayan state of India, and more than 80 percent of its area falls under the hilly region [1]. The state has extended forest cover, located at high altitude, and has deep glacier mass at the high altitude area of the state [2]. This geographical location of the state has made it more vulnerable to climate change [3-4].

https://doi.org/10.35762/AER.2021.43.1.1

As has been observed, the state is highly affected by frequent flash floods and cloudburst during monsoon season, especially at high altitude areas. The historical data shows that the frequency of these events is increasing year after year. As per the report of the Inter-governmental Panel on Climate Change (IPCC) 2013-AR5, the predicted increase in temperature from the year 1990 to 2100 will be approximately 1.4°C to 5.8° C, which will melt the glaciers of the state [5–6]. The report also said that the change in local precipitation and temperature due to climate change might increase the hazards like droughts and floods as well as it may increase their severity [7-8]. Therefore, there is a need to study the spatio-temporal change of rainfall of the state. So that appropriate adaptation policies can be taken up to mitigate the impact.

In recent years, different groups of researchers and scientists around the world are using General Circulation Model (GCM) models to predict the possible changes that may occur due to climate change [9]. The GCM models are capable of predicting the expected change in climatic conditions for the future [5, 10–12]. However, the GCM models are producing results on a very large grid system, i.e., a grid size of 200 to 650 km [13]. Due to this large grid size, the results obtained are not precise enough to be used directly to study the variation of different hydrological impacts on a local scale [14]. To overcome these scale parameters, the downscaling methods which are capable of filling the rift among the local scaled climatic inputs and global scaled climatic parameters can be used [15–17].

The downscaling is a procedure that relates local and regional scale climate variables to the larger-scale atmospheric components, *i.e.*, downscaling joins the gap between large and local scale climatic data [18–19]. The downscaling is necessary as the GCM outputs are of insufficient spatial resolution, causing an insufficient representation of orography and land surface characteristics. The normal spatial interoperation may not represent the features that may have important impacts on the local climate. The scale mismatch problem can be overcome by using Regional Climate Model (RCM) or by using the Statistical Downscaling techniques [2, 20–22]. The RCM develops a finer resolution regional climate model that is driven by boundary conditions simulated by the global GCMs at coarser scales. But the RCM is computationally costly and time-consuming [18, 23]. On the other hand, the statistical downscaling models derive a relationship between the large-scale atmospheric fields and local variables [5]. The model is simple in nature and can be implemented with less computational effort. As such, this study uses the statistical downscaling technique.

The statistical downscaling model can be developed by using the regression-based model. Linear and non-linear based regression models have been used to map the relationship between the large-scale atmospheric fields and local variables [24]. On the other hand, the artificial neural network (ANN) is one of the simplest but robust models for mapping the non-linear relation between the input and output variables. The ANN is considered to be a better model than the non-linear regression model as it can capture the hidden non-linearity between the input and output patterns. As such, the study uses the ANN model to develop the statistical downscaling model.

Data and model

The second-generation Canadian Earth System Model (CanESM2) is the fourth generation coupled global climate model developed by the Canadian Centre for Climate Modelling and Analysis (CCCma) of Environment and Climate Change Canada. CanESM2 represents the Canadian contribution to the IPCC Fifth Assessment Report (AR5). This CanESM2 model is a combination of the CanCM4 model and the Canadian Terrestrial Ecosystem Model (CTEM),

which based on the terrestrial carbon cycle [25]. The CTEM model explains the land-atmosphere carbon transaction phenomena. CanESM2 consists of three scenarios: RCP2.6, RCP4.5, and RCP8.5. The RCP (Representative Concentration Pathways) are four greenhouse gas concentration (not emissions) trajectories selected by the IPCC for its Fifth Assessment Report (AR5) [23, 26]. The four RCPs, RCP2.6, RCP4.5, RCP6.0, and RCP8.5, are described after a reasonable range of radiative forcing values projected in the year 2100. The RCP scenarios, i.e., RCP2.6, RCP4.5, RCP6, and RCP8.5, are labeled after a possible range of radiative forcing value of 2.6, 4.5, 6, and 8.5 W m^{-2}, respectively by the year 2100. The different RCP scenarios considered in this study are RCP2.6 RCP4.5 and RCP8.5. RCP represents a broad area of possible problems related to climate change like the effect of greenhouse gases, air pollutants, and their emissions and different land-use scenario. RCP8.5 consider the highest, and RCP2.6 consider the lowest scenarios of greenhouse gases. In this study, we have used the CanESM2 model. The location of the GCM point at Uttarakhand is shown in Supplementary Material (SM) 1.

There are 26 numbers of atmospheric variables available in the CanESM2 model, as shown in SM 2. The Principal Component Analysis (PCA) has been carried out to reduce the dimensionality of the data set. Principal component analysis, also recognized as the Karhunen Loeve transform, is one of the commonly accepted techniques for reducing the dimensionality [27–28]. The PCA converts a set of correlated M-dimensional predictors into a set of N-dimensional uncorrelated vectors, called principal components, by using a linear combination. During transformation, it is necessary to maintain that maximum information captured by the original data set is saved in the first few dimensions of the new set. SM3 shows the score of different predictor after the principal component analysis. In the present study, PCA was done to decrease the dimensionality of the predictors from 26 to the 6 (the selected variables are arbitrary and cannot be identified by their name), which contains the 99.978% information of the original data in the form of scores (SM 3). The correlation matrix verifies that the 1000 hPa wind speed, 1000 hPa wind direction, total precipitation, mean temperature at 2 m, specific humidity at 850 hPa, specific humidity at 500 hPa, 500 hPa wind direction, 500 hPa divergence are the major predictors with high correlation with predictand. The new data set is much lesser in size than the original set, and have the descriptions for nearly all of the specimen variance. This dataset is used as input to the statistical downscaling model. SM 4 shows the correlation between predictors before PCA, and SM 5 shows the correlation between predictors after PCA.

The Indian Metrological Department (IMD) gridded data, from 1961 to 2005 is used for historical rainfall data for all the nine districts of Uttarakhand. The IMD data is available at 0.25 × 0.25 grid size, as shown in SM 6.

Methodology

1) Study area

Uttarakhand is located in the great Himalayas, lies between 28043’ and 31027’N latitudes and 77034’ and 81002’E longitudes (Figure 1). The state spread in about 53,483 km^2 of the geographical area. Out of the total geographical area, mountains and hills cover about 46,035 km^2 of the area. Along with natural beauty, the state is also famous for natural calamities, such as cloudbursts, landslides, and flash floods.

Figure 1 Location map of the study area.

2) Data used

2.1) Rainfall data

Uttarakhand encounters massive precipitation, especially from June to August, i.e., monsoon season, in the form of flash flood due to its location at high altitude. Generally, the climate of the Uttarakhand is cold, with a high wind velocity during the year. As per the rainfall data collected from the IMD for all the thirteen districts of Uttarakhand, the normal annual rainfall of the state is about 1800 mm. The monthly average rainfall in all hilly districts are shown in SM 7, which represents the variation of average rainfall from 1150 mm to 600 mm in different districts of Uttarakhand.

Table 1 shows the location of the rain gauge stations, their altitudes, and the extent of data available for training, testing, and validation of the ANN model.

The working of the PCA-ANN approach has been shown in SM 8, and the standard procedure of downscaling is shown in Figure 2. Figure 3 shows the working chart for down-scaling using ANN. As shown in Figure 2 and Figure 3, firstly, we established a relationship between observed and large scale data, *i.e.*, predictands and predictors, respectively. Here, the rainfall is predictand, and GCM data is the predictor. The selection of predictors has been performed using PCA. The selected predictands and historical rainfall data have been used to calibrate and validate the model. This validated model, *i.e.*, the ANN model, is used to predict the rainfall under different RCP scenarios, as explained in Figure 2.

Table 1 Data used for calibration and validation of the ANN Model

Station Name	Longitude (degree), N	Latitude (degree), E	Altitude (m)	Data used to develop ANN model (Period)	GCM used
Uttarkashi	78.44	30.72	1158	1961-2005	CanESM2
Chamoli	79.55	30.56	6967	1961-2005	CanESM2
Tehri Garhwal	78.48	30.33	1750	1961-2005	CanESM2
Almora	29.58	79.64	1642	1961-2005	CanESM2
Bageswar	29.84	79.64	1004	1961-2005	CanESM2
Champawat	29.33	80.09	1615	1961-2005	CanESM2
Pauri	30.13	78.77	1814	1961-2005	CanESM2
Pitthoragarh	29.58	80.21	1514	1961-2005	CanESM2
Rudraprayag	30.28	78.98	895	1961-2005	CanESM2

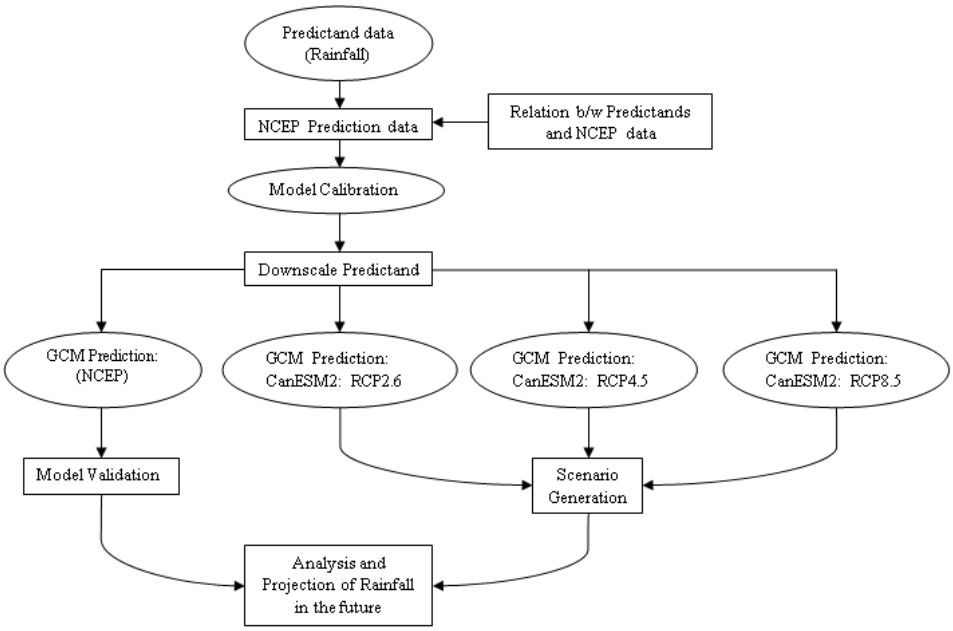

Figure 2 The flowchart of the downscaling process.

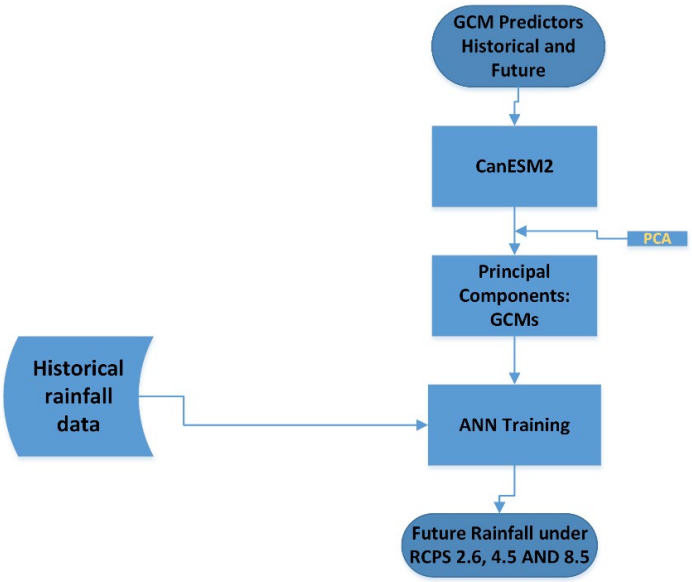

Figure 3 The working chart for downscaling using ANN.

3) Artificial Neural Network (ANN) model for downscaling

Artificial Neural Networks (ANNs), along with PCA, has been applied to develop the downscale model. The Feed Forward Back Propagation (FFBP) algorithm is used to develop a multi-layer perceptron (MLP) ANN model for downscaling of precipitation in the nine hilly districts of Uttarakhand.

An artificial neural network (ANN) is a knowledge processing method based on the different data which has a similar comparable function as neurons of the human brain [29–30]. MLPs are the commonly accepted and the simplest type of ANN model [31]. The MLPs are used to derive the relationship between different inputs and outputs [4, 32]. The multi-layer perceptron is feed-forward networks that comprise one or more hidden layers, as shown in SM 8. The MLP used in the present study consist of three layers, i.e., an input layer, a hidden layer, and an output layer. The model is trained using the Levenberg–Marquardt (LM) algorithm (Levenberg, 1944; Marquardt, 1963), which is an effective learning strategy for multi-layer feed-forward networks [33–34]. This method is a revised variant of the classic Newton approach for obtaining an optimum result for any optimization problem.

The parameters used in the ANN model are given in Table 1 and Table 2. There are six inputs to the model, as obtained from the principal component analysis. The only output from the model is the rainfall. An experiment has been conducted to find the number of neurons in the hidden layer. The experiment shows that the model is providing the best performance when the number of neurons in the hidden layer is 12.

4) Statistical evaluators

The different statistical parameters are used for the performance evaluation of the models [35–36]. In the present study, RMSE, R^2, and NSE are used to verify the results of the ANN model during the calibration and validation process, as given in Eq. 1, 2, and 3, respectively.

4.1) Root mean square error (RMSE)

The root-mean-square deviation (RMSD) or root-mean-square error (RMSE) is commonly used to measure the deviations between sample or population values predicted by a model and the observed values [37]. The RMSE value can be obtained by using Eq. 1.

$$RMSE = \sqrt{\frac{\sum_{i=1}^{n}(X_{obs,i} - X_{model,i})^2}{n}} \quad \text{(Eq. 1)}$$

Where X_{obs} is the observed value, and X_{model} is the model predicted value at time/place *i*.

Table 2 The parameters selected for the ANN downscaling model

ANN network type	Parameters	Name
MLP (Multi-layer perceptron: feed-forward networks)	Number of layers	3
	Neurons: Inputs: Hidden: Output:	 06 12 01
	Activation function	Sigmoid in the hidden layer Linear in the output layer
	Training algorithm	Levenberg-Marquardt

4.2) Coefficient of determination (R^2)

The coefficient of determination (R^2) shows the intensity and control of a linear relationship between two variables [38]. The correlation is +1 in the case of a perfect increasing linear relationship, and -1 in case of a decreasing linear relationship. The R^2 value can be obtained by using Eq. 2

$$R^2 = \frac{[\sum_{i=1}^{n}(O_i-\overline{O_i})*(P_i-\overline{P_i})]^2}{[\sum_{i=1}^{n}(O_i-\overline{O_i})*\sum_{i=1}^{n}(P_i-\overline{P_i})]} \quad \text{(Eq. 2)}$$

Where, O_i and P_i are observed and simulated value respectively, n is the total number of test data and $\overline{P_i}$, $\overline{O_i}$ are the mean value.

4.3) Nash-Sutcliffe coefficient (E)

The Nash-Sutcliffe model efficiency coefficient (E) is commonly used to assess the predictive power of hydrological discharge models [5, 39]. It is defined as Eq. 3.

$$E = 1 - \frac{\sum_{i=1}^{n}(X_{obs,i} - X_{model})^2}{\sum_{i=1}^{n}(X_{obs,i} - \overline{X_{obs}})^2} \quad \text{(Eq. 3)}$$

Where X_{obs} is the observed value, and X_{model} is the model predicted value at time/place *i*. Nash-Sutcliffe efficiencies can range from -∞ to 1. An efficiency of 1 (E = 1) corresponds to a perfect match between model and observations.

Results and discussions

1) Graphical analysis of ANN model during calibration and validation

After the selection of predictors and predictands, the ANN model is calibrated and validated using the historical datasets. In the case of any missing rainfall data in the IMD database, the linear interpolation method is used to find the missing data. As discussed earlier, the PCA is applied to select the predictor to train the ANN model. The first seven principal components, *i.e.*, predictors, are used in the analysis, which covers 99.77% of the predictor data property. For developing the ANN model, 70% of data is used for training purposes, and the remaining 30% is used for testing and validation.

The graphical representation of ANN predicted and observed precipitation data had been shown in SM 9 and SM 10 in the form of scatterplot and bar diagram. The scatterplots between observed and ANN predicted monthly precipitation for both the calibration and validation period for all the hilly regions are satisfactory since the R^2 value is ranging from 0.79 to 0.9. The bar diagram between ANN and actual precipitation shows the better-predicting capability of the ANN model. Along with the graphical representation, various statistical parameters were also used to analyze the results. The value of the statistical parameters is shown in Table 3. The statistical parameters also validate the ANN model performance, as in most of the hilly districts, the R^2 value is more than 0.8 during both calibration and validation phase except for Champawat and Rudraprayag. The Nash coefficient (E), is also approaching one except for Champawat and Pauri districts for both the phases, *i.e.*, calibration and validation.

The analysis of the results shows that the ANN model, combined with the PCA for the selection of predictors, is suitable for the statistical downscaling of the GCM data. Based on the ANN model, we performed the scenario analysis, *i.e.*, the rainfall has been predicted for the three RCPs, *i.e.*, RCP2.6, RCP4.5, and RCP8.5.

Table 3 Statistical parameters used for the model performance evaluation in terms of RMSE, R^2, and E for the ANN model in all nine hilly districts of Uttarakhand

Station/ Districts name	Parameters in the training phase			Parameters in validation phase		
	R^2	RMSE	E	R^2	RMSE	E
Almora	0.84	11.00	0.45	0.85	15.00	0.83
Bageswar	0.80	2.07	0.75	0.73	2.95	0.66
Chamoli	0.88	12.61	0.84	0.89	12.69	0.82
Champawat	0.70	2.02	0.49	0.65	2.15	0.59
Pauri Garhwal	0.84	2.39	0.33	0.92	2.29	0.35
Pitthoragarh	0.79	1.86	0.72	0.85	2.11	0.83
Rudraprayag	0.72	1.85	0.63	0.86	1.98	0.80
Tehri Garhwal	0.84	17.00	0.81	0.91	16.35	0.86
Uttarkashi	0.80	19.49	0.73	0.85	14.91	0.83

2) Scenario analysis for the RCPs 2.6, 4.5 and 8.5

For predicting the effect of climate change on precipitation trends CanESM2 GCM scenario, *i.e.*, RCP2.6, RCP4.5, and RCP8.5, were used. The period from 1961–2000 is selected as the baseline period to evaluate the change in rainfall. The selection of the baseline period is based on the procedure mentioned in the literature that 40 years of data is sufficient to assess the transformation in climate. So, the prediction of future rainfall is based on the comparison of these two-time extents, *i.e.*, 1961–2000 and 2005–2100. After calibration and validation of ANN model, the model is used to downscale the large-scale predictor variables derived from the RCP2.6, RCP4.5, and RCP8.5 scenarios of CanESM2, with daily precipitation simulated for the following periods: historical (1961–2000), the 2020s (2005–2021), 2050s (2022–2051), 2080s (2052–2080) and 2100s (2081–2100). As mentioned above, the historical simulation (1961–2000) acts as a reference for future projection and changes. Predicted changes in annual mean precipitation during future periods, *i.e.*, 2020, 2050, 2080, and 2100, in all nine hilly regions of Uttarakhand are shown in Figure 4 and Table 4, which shows a mixed pattern of positive or negative changes, with different trends in 2020 and 2050, and steady with the increases in 2080 and 2100. The trend shows that as compared to the baseline period, the amount of rainfall will increase significantly in all nine basins of Uttarakhand between 2081 to 2100 due to the change in the climate. While there is a mixed trend in rainfall, under CanEsm2 scenarios of RCP2.6 and RCP 4.5. The fluctuation in rainfall is slightly different for two scenarios, *i.e.*, RCP2.6 and RCP4.5, as compared to the worst emission scenario of RCP8.5. For RCP2.6, the up to 2080, sometimes the rainfall has an increasing trend, and in some decades, it has a decreasing trend. For RCP4.5, the increasing trend is slightly higher than the baseline period for 2020 and 2050, and in 2080 and 2100. For quantifying the variation in rainfall, we calculated the percentage of bias (PBIAS) or % change with respect to the historical data. The % change or PBIAS measures the average tendency of the predicted data to be larger or smaller than their observed counterparts. The optimal value of PBIAS is 0.0, with low magnitude values indicating an accurate model simulation. Positive values indicate underestimation bias, and negative values indicate over-estimation bias. The PBIAS is calculated as Eq. 4.

$$PBIAS = \frac{(y_i - x_i)}{x_i} \times 100 \qquad \text{(Eq. 4)}$$

Where y_i is the predicted value and x_i is the observed value.

Based on the % change value, the approximate predicted change up to the 21st century would be varying up to 21% in hilly regions of Uttarakhand under the scenarios of RCP8.5 (Figure 4).

3) Seasonal variation of rainfall: trend analysis

For the monsoon season, *i.e.*, for June, July, August, and September, the rainfall has been plotted with respect to the projected scenario. In other words, a comparative diagram has been plotted between historical and different scenarios rainfall for the Uttarakhand hilly areas cumulatively and shown in Figure 5. The graph shows an increase of around 200% in rainfall for the RCP8.5 and approximately 180% for RCP4.5 with respect to the historical monsoon rainfall data. In the case of RCP 2.6, there is not so much variation in rainfall; the rainfall is similar to the historical rainfall. The volume of rainfall has also projected a shift from August to September in the case of RCP8.5, as shown in Figure 6. *i.e.*, a shift was observed in the seasonal rainfall (*i.e.*, monsoon rainfall of a year). In other words, precipitation in the early months of the monsoon will reduce in the future while there may be an increased rainfall in the last month, *i.e.*, around September.

Table 4 Projected future changes of annual mean precipitation in the all nine hilly districts of Uttarakhand

Scenario	RCP2.6				RCP4.5				RCP8.5			
Timeline	**2020**	**2050**	**2080**	**2100**	**2020**	**2050**	**2080**	**2100**	**2020**	**2050**	**2080**	**2100**
Chamoli	-1.69	-0.33	4.73	5.25	1.02	-1.78	7.07	8.59	5.82	5.38	9.27	19.51
Uttarkashi	-0.22	1.25	-1.89	4.66	1.3	4.81	6.13	8.09	8.03	11.39	12.53	21.5
Tehri	-1.08	2.7	1.53	5.05	1.05	2.8	5.17	10.7	4.32	9.18	10.85	15.99
Almora	0.02	0.41	1.32	2.54	0.44	2.07	4.11	6.45	4.22	6.44	9.45	15.35
Bageswar	0.42	0.66	1.47	2.78	0.49	1.47	2.33	7.23	6.54	6.98	10.12	17.85
Champawat	0.37	0.23	1.06	1.96	1.04	2.44	3.42	8.44	4.98	5.23	9.87	13.22
Pauri Garhwal	-0.12	-0.24	0.49	1.34	1.54	2.13	2.33	6.96	7.26	6.98	9.61	19.64
Pitthoragarh	-0.2	0.29	0.67	2.01	1.11	1.78	3.73	4.56	5.87	7.12	11.45	20.23
Rudraprayag	0.04	0.11	0.94	1.94	1.64	1.97	3.61	5.81	7.23	7.77	11.92	19.84

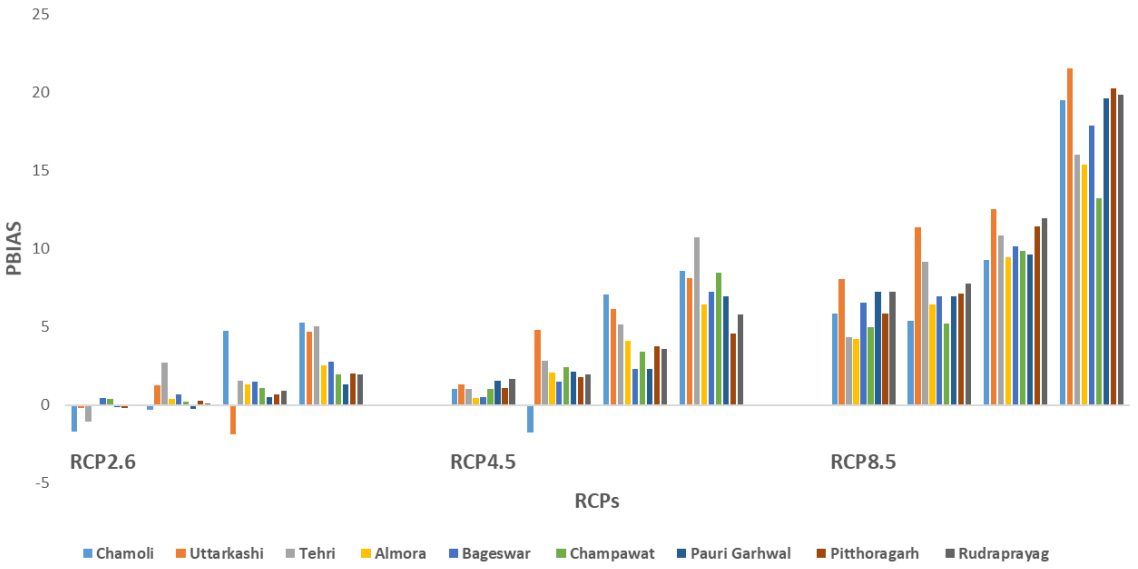

Figure 4 Showing PBIAS under different scenarios.

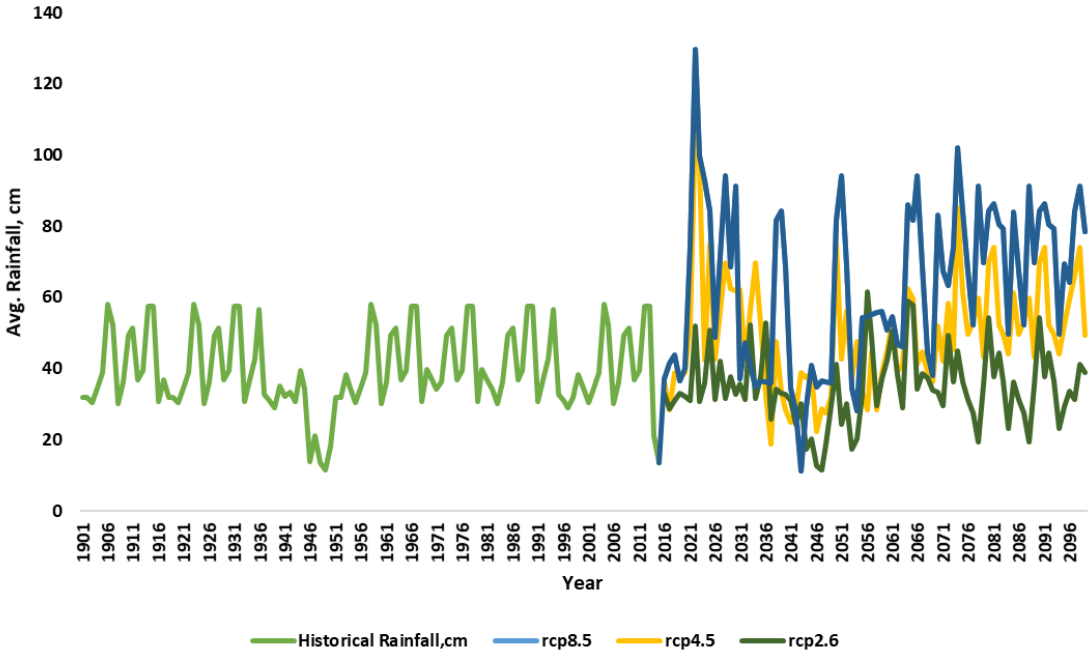

Figure 5 Projection of rainfall under different scenarios for monsoon season (June-July-August-September) with respect to the historical data.

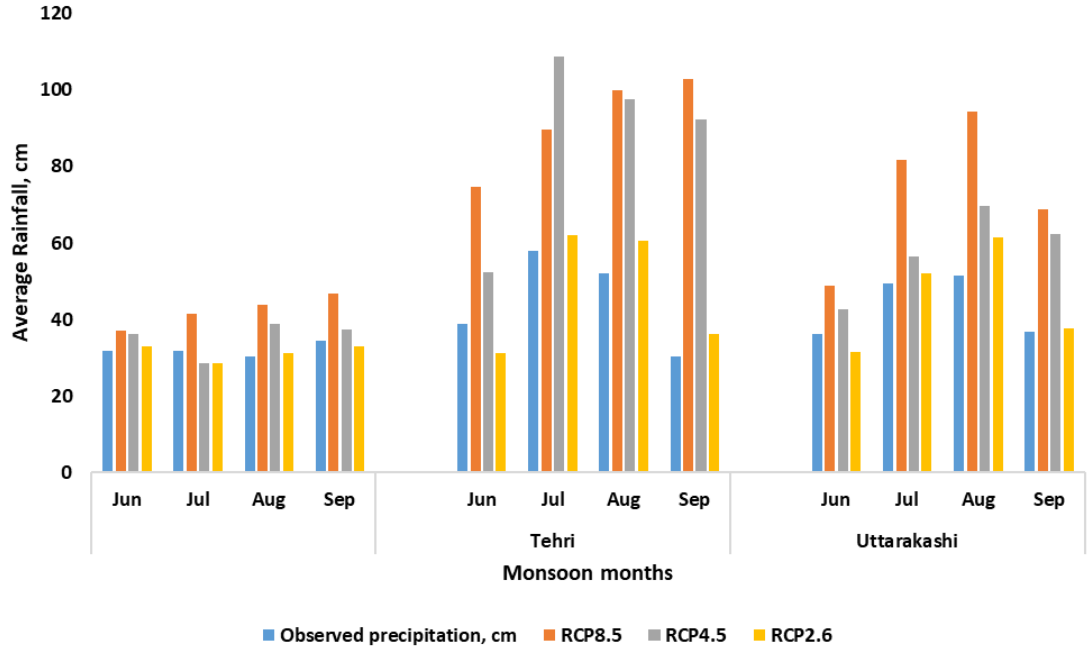

Figure 6 Projection of rainfall for three regions for the monsoon season (June-July-August-September) with respect to the historical data.

Conclusions

The rainfall in hilly districts of Uttarakhand is following a steadily increasing trend in the case of RCP4.5 and RCP8.5 scenarios. In reverse, the trend in the case of RCP2.6 follows a mixed type. There was an apparent indication of climate change in upper Himalayan districts like Pithoragarh, Rudraprayag, and Chamoli, which was observed from the peak of monthly rainfall. The percentage change in monsoon rainfall may go up to 200% in the case of RCP8.5 in comparison with the observation data. Also, the

volume of rainfall may increase in the case of RCP8.5 between July to September as compared to the historical data, i.e., there may be a shift of monsoon rainfall in the future. The present study is conducted under different constraints like missing rainfall data, etc. which may affect the projection of rainfall. Further, snowmelt has not been considered in the study. Overall, the present study is providing an enhanced knowledge of climate change appraisal in the hilly regions of Uttarakhand. The outcomes are relevant in the formulation of water resources and environmental policies in the state. However, further research studies have to be carried out, incorporating the different GCMs and investigate other features, such as the effect of climate change on base flow, temperature fluctuation, etc. The findings of this study are in line with the conclusions made by [40], where it has been stated that there may be a shift in future monsoon rainfall, and there is a rising trend of rainfall over the Himalayan foothill.

Conflict of Interest: None

References

[1] Mishra, A. Changing climate of Uttarakhand, India. Journal of Geology and Geophysics, 2014, 3(4), 1–5.

[2] Mathison, C., Wiltshire, A.J., Falloon, P, Challinor, A.J. South Asia river flow projections and their implications for water resources. Hydrology and Earth System Sciences Discuss, 2015, 12(6), 5789–5840.

[3] Scanlon, B.R., Döll, P., Longuevergne, L., Global models underestimate large decadal declining and rising water storage trends relative to GRACE satellite data. Proceedings of the National Academy of Sciences, 2018, 115(6), E1080–E1089.

[4] Pervez, MS., Henebry, GM. Projections of the Ganges-Brahmaputra precipitation-downscaled from GCM predictors. Journal of Hydrology, 2014, 517, 120–134.

[5] Chen, H., Xu, C-Y., Guo, S. Comparison and evaluation of multiple GCMs, statistical downscaling and hydrological models in the study of climate change impacts on runoff. Journal of Hydrology, 2012, 434, 36–45.

[6] Crawford, T., Betts, N.L., Favis-Mortlock, D. GCM grid-box choice and predictor selection associated with statistical downscaling of daily precipitation over Northern Ireland. Climate Research, 2007, 34(2), 145–160.

[7] Randall, D.A., Wood, R.A., Bony, S. Climate models and their evaluation. *In:* Manzini, E., Matsuno, T., McAvaney, B. Climate change 2007: The physical science basis. Contribution of Working Group I to the Fourth Assessment Report of the Intergovernmental Panel on Climate Change. New York: Cambridge University Press, 2007, 591–662.

[8] Cardona, O.D., van Aalst, M.K. Determinants of Risk: Exposure and Vulnerability. *In:* Décamps, H., Keim, M. Managing the risks of extreme events and Disasters to advance climate change adaptation. A Special Report of Working Groups I and II of the Inter-governmental Panel on Climate Change (IPCC). New York: Cambridge University Press, 2012, 65–108.

[9] Xu, R., Chen, N., Chen, Y., Chen, Z. Downscaling and projection of multi-CMIP5 precipitation using machine learning methods in the upper Han River Basin. Advances in Meteorology, 2020, 1–17.

[10] Rajan, S. Statistical downscaling of GCM output, hydrological simulation and generation of future scenario using variable infiltration capacity (vic) model for the Ganga Basin, India. 2014, (Vic), 132.

[11] Shukla, R., Khare, D., Deo, R. Statistical downscaling of climate change scenarios of rainfall and temperature over Indira Sagar canal command area in Madhya Pradesh, India. Proceedings - 2016 IEEE 14th International Conference on Machine Learning and Applications, ICMLA 2016. 2016, 313–317.

[12] Pichuka, S., Prasad, R.R., Maity, R., Kunstmann, H. Development of a method to identify change in the pattern of extreme streamflow events in future climate: Application on the Bhadra Reservoir inflow in India. Journal of Hydrology: Regional Studies, 2017, 9, 236–246.

[13] Tan, M.L., Ibrahim, A.L., Yusop, Z., Chua, V.P., Chan, NW. Climate change impacts under CMIP5 RCP scenarios on water resources of the Kelantan River Basin, Malaysia. Atmospheric Research, 2017, 189, 1–10.

[14] Huang, J., Zhang, J., Zhang, Z., Xu, C., Wang, B., Yao, J. Estimation of future precipitation change in the Yangtze River basin by using statistical downscaling method. Stochastic Environmental Research and Risk Assessment. 2011, 25(6), 781–792.

[15] Mahmood, R., Babel, M.S. Future changes in extreme temperature events using the statistical downscaling model (SDSM) in the trans-boundary region of the Jhelum river basin. Weather and Climate Extremes. 2014, 5(1), 56–66.

[16] Wilby, R.L., Dawson, C.W. Statistical down-scaling model-decision centric (SDSM-DC) Version 5.2 Supplementary Note. 2015.

[17] Wilby, R., Dawson, C., Barrow, E. SDSM — A decision support tool for the assessment of regional climate change impacts. Environmental Modelling and Software, 2002, 17(2), 145–157.

[18] Barman, S., Bhattacharjya, R.K. ANN-SCS Based Hybrid Model in Conjunction with GCM to Evaluate the Impact of Climate Change on the Flow Scenario of River Subansiri. Journal of Water and Climate Change, 2019, jwc2019221, 1–15.

[19] Nourani, V., Razzaghzadeh, Z., Baghanam, AH., Molajou, A. ANN-based statistical downscaling of climatic parameters using decision tree predictor screening method. Theoretical and Applied Climatology, 2019, 137(3-4), 1729–1746.

[20] Bhatt, D., Mall, RK. Surface water resources, climate change and simulation modeling. Aquatic Procedia, 2015, 4(Icwrcoe), 730-738.

[21] Chu, X., Lin, Z., Nasab, MT. Macro-scale grid-based and subbasin-based hydrologic modeling: Joint simulation and cross-calibration. Journal of Hydroinformatics, 2019, 21, 77–91.

[22] Frappart, F., Ramillien, G. Monitoring groundwater storage changes using the Gravity Recovery and Climate Experiment (GRACE) satellite mission: A review. Remote Sensing, 2018, 10(6).

[23] Zhang, Y., You, Q., Chen, C., Ge, J. Impacts of climate change on streamflows under RCP scenarios: A case study in Xin River Basin, China. Atmospheric Research, 2016, 178–179, 521–534.

[24] Barman, S., Bhattacharjya, R.K. ANN-SCS-based hybrid model in conjunction with GCM to evaluate the impact of climate change on the flow scenario of the River Subansiri. Journal of Water & Climate Change, 2019, 1–5.

[25] Feyissa, G., Zeleke, G., Bewket, W., Gebremariam, E. Downscaling of future temperature and precipitation extremes in Addis Ababa under climate change. Climate. 2018, 6(3), 58.

[26] Kim, S., Kwak, J., Kim, H.S., Jung, Y., Kim, G. Nearest neighbor-genetic algorithm for downscaling of climate change data

from GCMs. Journal of Applied Meteorology and Climatology, 2016, 55(3), 773–789.

[27] Yang, P., Xia, J., Zhan, C., Qiao, Y., Wang, Y. Monitoring the spatio-temporal changes of terrestrial water storage using GRACE data in the Tarim River basin between 2002 and 2015. Science of the Total Environment, 2017, 595, 218–228.

[28] Beaumont, R. An introduction to principal component analysis & factor analysis using SPSS 19 and R (psych package). Journal of Geophysical Research, 2012. [Online] Available from: http://www.floppybunny.org/robin/web/virtualclassroom/stats/statistics2/pca1.pdf.

[29] Kumar, D., Bhishm, S.K., Khati S. Black box model for flood forecasting. Journal of Civil Engineering 2012, 40, 47–59.

[30] Hannan, S.A., Manza, R.R., Ramteke, R.J. Generalized regression neural network and radial basis function for heart disease diagnosis. International Journal of Computer Applications, 2010, 7(13), 7–13.

[31] Joshi, R. Artificial Neural Network (ANN) based empirical interpolation of precipitation. International Journal of Mathematical, Engineering and Management Sciences, 2016, 1(3), 93–106.

[32] Ghosh, S., Misra, C. Assessing hydrological impacts of climate change: Modeling techniques and challenges. Open Hydrology Journal, 2010, 4, 115–121.

[33] Kusunoki, S., Arakawa, O. Are CMIP5 models better than CMIP3 models in simulating precipitation over East Asia? Journal of Climate, 2015, 28(14), 5601–5621.

[34] Onyutha, C., Tabari, H., Rutkowska, A., Nyeko-Ogiramoi, P., Willems, P. Comparison of different statistical downscaling methods for climate change rainfall projections over the Lake Victoria basin considering CMIP3 and CMIP5. Journal of Hydro-environment Research, 2016, 12, 31–45.

[35] Bera, S. Trend analysis of rainfall in Ganga Basin, India during 1901-2000. American Journal of Climate Change, 2017, 6(1), 116–131.

[36] Pricope, N.G., Halls, J.N., Rosul, L.M., Hidalgo, C. Residential flood vulnerability along the developed North Carolina, USA coast: High resolution social and physical data for decision support. Data in Brief. 2019, 24, 103975.

[37] Xiao, R., He, X., Zhang, Y., Ferreira, V.G., Chang, L. Monitoring groundwater variations from satellite gravimetry and hydrological models: A comparison with in-situ measurements in the mid-Atlantic region of the United States. Remote Sensing, 2017, 1, 686–703.

[38] Kazmi, D.H., Rasul, G., Li, J., Cheema, S.B. Comparative study for ECHAM5 and SDSM in downscaling temperature for a geo-climatically diversified region, Pakistan. Applied Mathematics, 2014, 5, 137–143.

[39] Moriasi, D.N., Arnold, J.G., Van Liew, M.W., Bingner, Harmel, R.L., Veith, T.L. Model evaluation guidelines for systematic quantification of accuracy in watershed simulations. Trans ASABE. 2007, 50(3), 885–900.

[40] Banerjee, A., Dimri, A.P., Kumar, K. Rainfall over the Himalayan foot-hill region: Present and future. Journal of Earth System Science, 2020, 129.